

First stars, very massive black holes and metals

R. Schneider¹, A. Ferrara¹, P. Natarajan^{2,3}, and K. Omukai^{1,4}

¹ Osservatorio Astrofisico di Arcetri, Largo Enrico Fermi 5, 50125 Firenze, Italy

² Department of Astronomy, Yale University, New Haven, CT 06520-8101, USA

³ Yale Center for Astronomy and Astrophysics, Yale University, New Haven, CT 06511,
USA

⁴ Division of Theoretical Astrophysics, National Astronomical Observatory, Mitaka, Tokyo
181-8588, Japan

Received _____; accepted _____

ABSTRACT

Recent studies suggest that the initial mass function (IMF) of the first stars was likely to be extremely top-heavy, unlike what is observed at present. We propose a scenario to generate fragmentation to lower masses once the first massive stars have formed and derive constraints on the primordial IMF. We estimate the mass fraction of pair-unstable supernovae, shown to be the dominant sources of the first heavy elements. These metals enrich the gas up to $\approx 10^{-5} Z_{\odot}$, when a transition to efficient cooling-driven fragmentation occurs producing $\lesssim 1 M_{\odot}$ clumps. We argue that the remaining fraction of the first stars ends up in $\approx 100 M_{\odot}$ VMBHs (Very Massive Black Holes). If we further assume that all these VMBHs are likely to end up in the centers of galactic nuclei constituting the observed SMBHs, then $\approx 1\%$ of the first stars contributed to the initial metal enrichment and the IMF remained top-heavy down to a redshift $z \approx 10$. Interestingly, this is the epoch at which the cool metals detected in the Ly α forest at $z \approx 3$ must have been ejected from galaxies. At the other extreme if none of these VMBHs have as yet ended up in SMBHs, we expect them to be either (i) en-route towards galactic nuclei thereby accounting for the X-ray bright off-center sources detected locally by ROSAT or (ii) as the dark matter candidate composing the entire baryonic halos of galaxies. For case (i) we expect $\approx 90\%$ of the primordial stars to produce metals causing the transition at a redshift of $\gtrsim 16$, and for case (ii) $\lesssim 10^{-5}$ - a very negligible fraction of the initial stars produce the metals and the transition redshift occurs at $z_f \gtrsim 2$. In this paper we present a framework (albeit one that is not stringently constrained at present) that relates the first episode of star formation to the fate of their remnants at late times. Clearly, further progress in understanding the formation and fragmentation of Population III stars within the cosmological

context will provide tighter constraints in the future. We conclude with a discussion of several hitherto unexplored implications of a high-mass dominated star formation mode in the early Universe.

Subject headings: galaxies: formation - intergalactic medium - black holes - cosmology: theory

1. Introduction

Recent studies have started to tackle the formation and collapse of the first cosmic structures (often referred to as PopIII objects) through numerical simulations (Abel *et al.* 1998; Bromm, Coppi & Larson 1999, 2001; Abel, Bryan & Norman 2000; Bromm *et al.* 2001) based on hierarchical scenarios of structure formation. These studies have shown that gravitational collapse induces fragmentation of pre-galactic units with an initial baryonic mass $\approx 10^5 M_\odot$ into smaller clumps with a typical mass of $10^3 M_\odot$, which corresponds to the Jeans mass set by molecular hydrogen cooling. However, a considerable mass range ($10^{2-4} M_\odot$) for the clumps seems plausible.

Tracking the subsequent gravitational collapse of these metal free clumps is a very challenging problem as it requires the simultaneous solution of hydrodynamics and of (cooling lines) radiative transfer (Omukai & Nishi 1998; Nakamura & Umemura 1999; Ripamonti *et al.* 2001). Preliminary attempts and several physical arguments indicate that these clumps do not fragment into smaller units as the evolution progresses to higher densities. Independent studies (Hernandez & Ferrara 2001) comparing the observed number of metal poor stars with that predicted by cosmological models, also imply that the characteristic stellar mass sharply increases with redshift. Hence, there are grounds to believe that the first stars were very massive.

The evolution of massive, metal free stars is currently subject to a rapidly growing number of studies (Fryer 1999; Fryer, Woosley & Heger 2001; Heger & Woosley 2001) which rejuvenate earlier activity (Fowler & Hoyle 1964; Carr, Bond & Arnett 1984; El Eid *et al.* 1983; Fricke 1973; Fuller *et al.* 1986). As we discuss in detail later in the paper, stars more massive than about $260 M_\odot$ collapse completely to black holes, therefore not contributing to the metal enrichment of the surrounding gas. Similar arguments apply to stars in a lower mass window ($30 M_\odot$ - $140 M_\odot$), which are also expected to end their

evolution as black holes. Hence, if supernovae from more standard progenitors (stellar masses in the range $8 M_{\odot}$ - $40 M_{\odot}$) are either not formed efficiently or occur in negligible numbers, it appears that the initial cosmic metal enrichment had to rely on the heavy element yield from the so-called pair-unstable supernovae ($\text{SN}_{\gamma\gamma}$), whose explosion leaves no remnant. This conclusion can potentially be tested by studying peculiar elemental abundances, for example of heavy *r*-process elements (Oh *et al.* 2001).

Metallicity is thought to noticeably affect the fragmentation properties of a gravitationally unstable gas. For example, Bromm *et al.* (2001) have shown that the evolution of a collapsing proto-galaxy depends strongly on the level of gas pre-enrichment. These authors argue that a critical metallicity $\approx 10^{-4} Z_{\odot}$ exists such that, above that value vigorous fragmentation into relatively low mass ($\approx 10 M_{\odot}$) clumps takes place, differently from what is discussed above under metal-free conditions.

The key question then concerns the interplay between the properties of the IMF and the metal enrichment of the gas. To better illustrate this, let us ideally suppose that the first stars are all formed – as suggested by numerical simulations – with masses above the $\text{SN}_{\gamma\gamma}$ mass threshold, thus leading to the formation of black holes. Then, because metals are completely swallowed by the latter, the gas retains its primordial composition and star formation continues in the high-mass biased mode. A solution to this "star formation conundrum" must evidently exist as at present stars form with a much lower characteristic mass ($\approx 1 M_{\odot}$).

In this paper, we describe in detail a possible solution to this conundrum utilizing various constraints: metal abundance patterns in clusters, the mass density of super-massive black holes, off-nuclear galactic X-ray sources and, to a more speculative extent, the nature of a particular class (optically hidden) of gamma-ray bursts - we attempt to infer the main properties of the early stages of cosmic star formation.

2. Fragmentation modes

In this Section, we focus on the first episode of star formation and discuss the relevant cooling criteria and timescales in detail. We work within the paradigm of hierarchical cold dark matter (CDM) models for structure formation, wherein dark matter halos collapse and the baryons in them condense, cool, and eventually form stars. Once a halo of mass M collapses at redshift of z_c , the baryons are shock-heated to the virial temperature given by

$$T_{\text{vir}} = 10^{4.5} \mu^{-1} M_8^{2/3} \left(\frac{1 + z_c}{10} \right) \text{ K}, \quad (1)$$

where $M_8 = M/10^8 h^{-1} M_\odot$ and μ is the molecular weight. If $T_{\text{vir}} \gtrsim 10^4$ K [or equivalently $M \gtrsim 10^9 (1 + z_c)^{-3/2} h^{-1} M_\odot$], the baryonic gas cools due to the excitation of hydrogen Ly α line. In the absence of metals, as expected for the very first episode of star formation, objects with $T_{\text{vir}} \lesssim 10^4$ K can cool only through the collisional excitation of molecular hydrogen. Hereafter, in this work, we refer to the former objects as Ly α -cooling halos and to the latter as PopIII objects.

The first stars form once the gas cools. The typical initial mass function (IMF) of this first generation of stars is still highly uncertain. Several authors have tackled this crucial issue through theoretical (Rees 1976; Rees & Ostriker 1977; Silk 1977, 1983; Haiman, Thoul & Loeb 1996; Uehara *et al.* 1996) and numerical approaches (Omukai & Nishi 1998; Nakamura & Umemura 1999, 2001; Abel, Bryan & Norman 2000; Bromm, Coppi & Larson 2001; Omukai 2000, 2001; Ripamonti *et al.* 2001). Recent multi-dimensional simulations of the collapse and fragmentation of primordial gas within PopIIIs, have reached convergence towards either a top-heavy IMF with typical masses of order $\gtrsim 10^2 M_\odot$ (Abel, Bryan & Norman 2000; Bromm, Coppi & Larson 2001) or a bimodal IMF with peaks at $\approx 10^2 M_\odot$ and $\approx 1 M_\odot$ (Omukai 2001). Note, that these numerical treatments cannot address the issue of the mass spectrum. Therefore, it is important to understand what physical processes set the scales of fragment masses and hence the stellar mass spectrum.

It is obvious that much hinges on the physics of cooling, primarily the number of channels available for the gas to cool and the efficiency of the process (Rees & Ostriker 1977). In general, cooling is efficient when the cooling time $t_{\text{cool}} = 3nkT/2\Lambda(n, T)$ is much shorter than the free-fall time $t_{\text{ff}} = (3\pi/32G\rho)^{1/2}$, i.e. $t_{\text{cool}} \ll t_{\text{ff}}$; where n (ρ) is the gas number (mass) density and $\Lambda(n, T)$ is the net radiative cooling rate [erg cm⁻³s⁻¹]. This efficiency condition implies that the energy deposited by gravitational contraction cannot balance the radiative losses; as a consequence, temperature decreases with increasing density. Under such circumstances, the cloud cools and then fragments. At any given time, fragments form on a scale that is small enough to ensure pressure equilibrium at the corresponding temperature, *i.e.* the Jeans length scale,

$$R_F \approx \lambda_J \propto c_s t_{\text{ff}} \propto n^{\gamma/2-1} \quad (2)$$

where the sound speed $c_s = (RT/\mu)^{1/2}$, $T \propto n^{\gamma-1}$, where γ is the adiabatic index. Since c_s varies on the cooling timescale, the corresponding R_F becomes smaller as T decreases. Similarly, the corresponding fragment mass is the Jeans mass,

$$M_F \propto n R_F^\eta \propto n^{\eta\gamma/2+(1-\eta)}, \quad (3)$$

with $\eta = 2$ for filaments and $\eta = 3$ for spherical fragments (Spitzer 1978). This hierarchical fragmentation process comes to an end when *(i)* cooling becomes inefficient or *(ii)* the gas becomes optically thick to cooling radiation; in both cases, at that juncture $t_{\text{cool}} \gtrsim t_{\text{ff}}$. At this stage, the temperature cannot decrease any further and it either remains constant (if energy deposition by gravitational contraction is exactly balanced by radiative losses) or increases. The necessary condition to stop fragmentation and start gravitational contraction within each fragment is that the Jeans mass does not decrease any further, thus favoring fragmentation into sub-clumps. From eq. 3, this implies the following condition:

$$\gamma \gtrsim 2 \frac{\eta - 1}{\eta}, \quad (4)$$

which translates into $\gamma \gtrsim 4/3$ for a spherical fragment and $\gamma \gtrsim 1$ for a filament. Thus, a filament is marginally stable and contracts quasi-statically when, $t_{\text{cool}} \approx t_{\text{ff}}$, and the gas becomes isothermal. Finally, when $t_{\text{cool}} \gg t_{\text{ff}}$ or the fragments become optically thick to cooling radiation, the temperature increases as the contraction proceeds adiabatically.

2.1. Fragmentation of metal-free clouds

In this subsection, we follow the evolution of metal-free primordial clumps during the fragmentation process. These results are based on the model of Omukai (2001). The gas within the dark matter halo is given an initial temperature of 100 K and the subsequent thermal and chemical evolution of the gravitationally collapsing cloud is followed numerically until a central proto-stellar core forms.

The gas within the dark matter halo gets shock-heated to the virial temperature T_{vir} , which is typically $\gg 100$ K. However, after a short transient phase (irrelevant for the present analysis), the evolutionary track in the (n, T) plane shown in Fig. 1 (top curve, upper panel) provides a good description of the thermal evolution of the gas. The metal-free gas is able to cool down to temperatures of a few hundred Kelvin regardless of the initial virial temperature. This is the minimum temperature at which molecular line cooling becomes effective.

The gas within halos with $T_{\text{vir}} > 10^4$ K starts to cool through the hydrogen Ly α line. It quickly reaches a temperature of ≈ 8000 K and, at this stage, the fraction of molecular hydrogen formed is sufficient to activate H₂ ro-vibrational line cooling. Thereafter, the gas within a Ly α -cooling halo follows the same thermal evolution as the gas within PopIIIs. Independent of the virial temperature, the thermal evolution of the gas rapidly converges to the (n, T) track corresponding to $Z = 0$ (the zero metallicity track), shown in Fig. 1. The

temperature of the gas decreases with increasing density, thus favoring fragmentation into sub-clumps.

As the number density increases, it reaches the critical value $n_{\text{cr}} \approx 10^3 \text{ cm}^{-3}$; and the corresponding Jeans mass is $\approx 10^4 M_{\odot}$ (empty dot in the upper panel of Fig. 1). The cooling time at this critical point becomes comparable to the free fall time as a consequence of the H_2 levels being populated according to LTE [regime where the cooling rate $\Lambda(n, T) \propto n$] and no longer according to NLTE [regime where $\Lambda(n, T) \propto n^2$]. The temperature then starts to rise slowly.

At this stage, the stability of the fragments toward further increase in the density needs to be investigated according to the condition eq. 4 above. The lower panel of Fig. 1 shows the density dependence of γ (see eq. 2) for each metallicity track. For a metal-free gas γ lies in the range $0 < \gamma - 1 < 1/3$, implying that further fragmentation is unlikely to occur unless the fragments are spherical. The only two deviations from the above range occur (see lower panel of Fig. 1) around $n = 10^{10} \text{ cm}^{-3}$ and 10^{16} cm^{-3} . The former is a result of the thermal instability due to three-body H_2 formation (Silk 1983; Haiman et al. 1996). However, this instability is quite weak and does not lead to fragmentation (Abel et al. 2000). The latter (at $n = 10^{16} \text{ cm}^{-3}$) is caused by H_2 collision-induced emission. This instability is also weak and probably unimportant.

It is important to stress that, even if the fragments are nearly spherical, fragmentation will be modest and is likely to result only in a low multiplicity stellar system. As the density increases, quasi-static contraction takes place ($n = 10^{20} \text{ cm}^{-3}$) until the fragments become optically thick to H_2 lines, $t_{\text{cool}} \gg t_{\text{ff}}$, and adiabatically collapse to increasingly higher central densities and temperatures. At this stage, $\gamma > 4/3$ and a central hydro-static core (stellar core, filled circle in Fig. 1, upper panel) is formed, with mass $\approx 10^{-3} M_{\odot}$ (Omukai & Nishi 1998).

We stress again that, as long as the gas is metal-free, these sequence of events and conclusions hold independent of the halo virial temperature, *i.e.* for PopIIIs as well as for Ly α -cooling halos. In Fig. 2 we show the evolution with temperature of the ionization fraction and of the fraction of molecular hydrogen for typical Ly α -cooling halos of mass $M = 10^8 M_\odot$ at three different redshifts, $z = 15, 20, 25$. We find that the evolution of these fractions is independent of the mass (or, equivalently, T_{vir}) and virialization redshift. Molecule formation in the post-shock flow which follows the virialization of the gas within a dark matter halo has been recently investigated by Uehara & Inutsuka (2000). If the gas is fully ionized, molecules form through non-equilibrium recombination, leading to overall fractions that are much higher than in the expanding homogeneous universe. As a consequence of enhanced H₂ and HD fractions, the gas rapidly cools to well below 10⁴ K and fragments. Molecular chemistry is important also for star formation in halos with $T_{\text{vir}} > 10^4$ K as recently assessed by Oh & Haiman (2001). They find that initial atomic line cooling leaves a large residual free electron density which allows molecule formation up to a universal fraction of $x_{\text{H}_2} = 10^{-3}$. The newly formed molecules cool the gas further to ~ 100 K and the gas fragments on mass scales of a few $100 M_\odot$.

Once the critical density for H₂ ($n_{\text{cr}} \approx 10^3 \text{ cm}^{-3}$ or 10^4 cm^{-3} for HD, if this is assumed to be the main coolant) has been reached, LTE conditions for the level populations disfavor further cooling and fragmentation. At this stage, fragments have masses comparable to the Jeans mass corresponding to the point $(n_{\text{cr}}, T_{\text{cr}})$ and virialize, following the evolution described above. Therefore, independent of the initial virial temperature, fragments are formed with typical masses $\approx 10^3 - 10^4 M_\odot$.

Each fragment is characterized by a central core of $10^{-3} M_\odot$ surrounded by a large envelope of gravitationally unstable gas. The core grows in mass due to gas accretion from the envelope. The mass of the formed stars depends on the accretion rate as well as

on the fragment mass (Larson 1999). In the absence of metals, radiation pressure cannot counter-balance mass accretion onto the core (Ripamonti *et al.* 2001) and the mass of the resulting star is comparable to that of the original fragment, *i.e.* $\lesssim 10^3 M_\odot$. We will return to this crucial issue in Section 2.3. The question that needs to be addressed now is what mechanism can finally lead to the transition to a conventional mode of star formation, *i.e.* to a standard IMF, and what are the necessary conditions for this to occur.

2.2. Fragmentation of metal-enriched clouds

We now consider the effects of the presence of heavy elements on the fragmentation process. Fig. 1 shows the effects of metal enrichment on the (n, T) tracks for the same initial conditions and different values of the mean metallicity.

In general, clouds with lower metallicity tend to be warmer because of their lower radiative cooling ability. As long as the clouds are transparent, cooling and fragmentation occur. Clouds with a mean metallicity $Z \approx 10^{-6} Z_\odot$ follow the same evolution as that of the gas with primordial composition in the (n, T) plane. However, at $Z \approx 10^{-4} Z_\odot$, H₂ formation on grain surfaces enhances cooling at low density. When the LTE-NLTE transition occurs for H₂, the cloud can still cool (though less efficiently) due to OI line cooling. At densities $> 10^6 \text{ cm}^{-3}$, heating due to H₂ formation becomes larger than compressional work, *i.e.* $\gamma > 1$ and the temperature starts to increase until thermal emission from grains due to energy transfer between gas and dust dominates the cooling. This occurs at a density $n \approx 10^{10} \text{ cm}^{-3}$, where the temperature drops to $\approx 100 \text{ K}$ and a new fragmentation phase occurs. This shows up in the lower panel of Fig. 1 as the large dip in the γ evolution. The minimum fragment mass is reached at the point indicated by the empty circle, when the density is $\approx 10^{13} \text{ cm}^{-3}$ and the corresponding Jeans mass is of order $10^{-2} M_\odot$. Finally, as the density increases, the gas becomes opaque to dust thermal emission, fragmentation

stops and compressional heating causes the fragments to contract adiabatically ($\gamma > 4/3$). Therefore, a critical metallicity of $Z_{\text{cr}} \approx 10^{-5} Z_{\odot}$ can be identified, which marks the transition point between metal-free and metal-rich gas evolution.

When the metallicity is $Z > 10^{-4} Z_{\odot}$, at density $\lesssim 10^4 \text{ cm}^{-3}$ cooling is driven by OI, CI and CO line emission. When the NLTE-LTE transition for the level populations of CO occurs, fragmentation stops and the temperature increases due to H_2 formation. The larger concentration of dust grains (assumed here to be proportional to the mean metallicity) leads to a significant thermal emission which is responsible for cooling the gas and starting a new phase of fragmentation. This stops when $T_{\text{grain}} \simeq T$ and thereafter the fragments contract quasi-statically until they become optically opaque to dust emission and adiabatic contraction occurs. Due to the enhanced ability to cool, fragmentation stops at lower temperatures and densities for higher metallicity clouds (see open circles in the lower panel of Fig. 1). However, the Jeans mass corresponding to the minimum fragmentation scale is always $10^{-2} M_{\odot} \leq M_F \leq 1 M_{\odot}$ for the metallicity range $10^{-4} \leq Z/Z_{\odot} \leq 1$, several orders of magnitude smaller than for a cloud with no metals.

At the onset of adiabatic contraction, when γ becomes larger than $4/3$, an initial hydro-static core forms (transient core) with a mass $\approx 10^{-2} M_{\odot}$ regardless of the metallicity of the gas. This transient core is fully molecular and is absent when the gas is metal-free. The temperature of the transient core increases as its mass increases due to accretion of surrounding gas. Eventually, the temperature reaches about 2000 K, where H_2 dissociation begins. This softens the equation of state until the dissociation is almost complete. Then, γ falls below $4/3$ in the density range $10^{16} - 10^{20} \text{ cm}^{-3}$. Note that the thermal evolution after H_2 dissociation (i.e., $n > 10^{16} \text{ cm}^{-3}$) is the same independent of the initial composition of the gas. After γ once again exceeds $4/3$, a hydro-static core (so-called stellar core) forms. Its physical characteristics are independent of metallicity ($n \approx 10^{22} \text{ cm}^{-3}$, $M \approx 10^{-3} M_{\odot}$;

Omukai 2000).

In this analysis, external sources of heating are not included. For example, if the collapsing gas is irradiated by a UV radiation field, two effects can be important for its energy balance, *i.e.* photoelectric heating and H₂ photo-dissociation. Both processes tend to stabilize the cloud equilibrium temperature to a higher value and to make it more isothermal so that fragmentation can be quenched at earlier stages. However, at redshifts prior to reionization the UV background field is relatively weak and inhomogeneous (Ciardi, Ferrara, & Abel 2000), hence we do not expect it to be important. Also note, that the CMB sets a lower limit to the temperature, $T = 2.73(1 + z)$ K. This is not relevant for clouds with $T > 100$ K (or $Z < 10^{-4}Z_{\odot}$) where the first stars presumably formed at redshifts $z < 30$; however, it might become an important constraint for the evolution of subsequent, more metal rich systems.

2.3. Formation of proto-stars

Proto-stars, whose mass is initially very low (about $10^{-3}M_{\odot}$), grow in mass by accretion of the envelope material. The final mass of stars is, then, determined not only by the mass of the fragments, but also by when accretion stops. The accretion rate onto the proto-star is related to the sound speed (and therefore, temperature) of the proto-stellar cloud by the relation, $\dot{M} \simeq c_s^3/G$, (Stahler, Shu, & Taam 1980).

As seen in Fig. 1, the temperature of proto-stellar clouds decreases with metallicity. Therefore, the mass accretion rate is higher for proto-stars formed from lower metallicity gas. If dust is present in the accretion flow, accretion onto the massive proto-star becomes increasingly difficult owing to the radiation pressure onto the dust. In present-day interstellar gas, accretion onto stars more massive than $30M_{\odot}$ is inhibited by this mechanism

(Wolfire & Cassinelli 1987). In gas with lower metallicity, the mass bound is expected to be higher because of the higher accretion rate and lower radiation force. In particular, for metal-free gas, this mechanism does not work. Therefore, without dust, accretion is likely to continue until the ambient gas supply is exhausted (Ripamonti *et al.* 2001).

In conclusion, the presence of metals not only enables fragmentation down to smaller mass scales $10^{-2}M_{\odot}$, but also breaks the one-to-one correspondence between the mass of the formed star and that of the parent fragment by halting the accretion through radiation force onto the dust.

3. The star formation conundrum

According to the scenario proposed above, the first stars that form within PopIII and Ly α -cooling halos out of gas of primordial composition tend to be very massive, with masses $\approx 10^{2-3}M_{\odot}$. It is only when metals change the composition of the gas that further fragmentation occurs producing stars with significantly lower masses. It is at this stage that we expect a transition to occur from a top-heavy IMF towards a more conventional IMF with a wide range of masses, such as the one observed locally (Scalo 1998, Kroupa 2001).

A growing body of observational evidence points to an early top-heavy IMF (see Hernandez & Ferrara 2000 and references therein). Compelling arguments for an early top-heavy IMF can also be made from observations on various scales: *(i)* the early enrichment of our Galaxy required to solve the so-called G-dwarf problem, *(ii)* the abundance patterns of metals in the Intraccluster Medium (ICM), *(iii)* the energetics of the ICM, *(iv)* the non-detection of metal-free stars, and *(v)* the over-production of low mass stars at the present epoch and metals at $z \sim 2 - 5$ for the submillimeter derived star formation histories using SCUBA detections for a standard IMF can be resolved with an

early top-heavy IMF.

For instance, the ICM metal abundances measured from Chandra and XMM spectral data are higher than expected from the enrichment by standard IMF SN yields in cluster galaxy members, which can be explained by a top-heavy early IMF. Furthermore, the observed abundance anomalies (*e.g.* oxygen) in the ICM can be explained by an early generation of PopIII SNe (Loewenstein 2001). There is observational evidence from the abundance ratio patterns of [Si/Fe], [Mg/Fe], [Ca/Fe] and [Ti/Fe] in the extremely metal-poor double-lined spectroscopic binary CS 22876-032 in the halo of our galaxy (Norris, Beers & Ryan 2000) for enrichment by a massive, zero-metallicity supernova on comparison with the theoretical models of Woosley & Weaver (1995). These issues, highly suggestive of top-heavy early star formation, have recently motivated a series of numerical investigations of the nucleosynthesis and final fate of metal-free massive stars (Heger & Woosley 2001; Fryer, Woosley & Heger 2001). In their recent paper, Heger & Woosley delineate three mass ranges characterized by distinct evolutionary paths:

1. $M_\star \gtrsim 260M_\odot$: the nuclear energy release from the collapse of stars in this mass range is insufficient to reverse the implosion. The final result is a very massive black hole (VMBH) locking up all heavy elements produced.

2. $140M_\odot \lesssim M_\star \lesssim 260M_\odot$: the mass regime of the pair-unstable supernovae (SN _{$\gamma\gamma$}).

Pre-collapse winds and pulsations result in little mass loss, the star implodes to a maximum temperature that depends on its mass and then explodes, leaving no remnant. The explosion expels metals into the surrounding ambient ISM.

3. $30M_\odot \lesssim M_\star \lesssim 140M_\odot$: black hole formation is the most likely outcome, because either a successful outgoing shock fails to occur or the shock is so weak that the fall-back converts the neutron star remnant into a black hole (Fryer 1999).

Stars that form in the mass ranges (1) and (3) above fail to eject most of their heavy elements. If the first stars have masses in excess of $260M_{\odot}$ (in agreement with numerical findings), they invariably end their lives as VMBHs (in the following we will refer to VMBHs as black holes of hundred solar mass or so) and do not release any of their synthesized heavy elements. However - as we have shown - as long as the gas remains metal-free, the subsequent generations of stars will continue to be top-heavy. This *star formation conundrum* can be solved only if a fraction of the first generation of massive stars have masses $\lesssim 260M_{\odot}$. Under such circumstances, these will explode as $\text{SN}_{\gamma\gamma}$ and enrich the gas with heavy elements up to a mean metallicity of $Z \gtrsim 10^{-5}Z_{\odot}$, and as per arguments outlined in the previous section (see Fig. 1), thereafter causing a shift over to an IMF that is similar to the local one. In what follows, we further explore the implications of the above scenario and derive the conditions for the solution of the conundrum.

3.1. Abundance of VMBHs and metals

As a consequence of the picture proposed above, VMBHs are an inevitable outcome. We now compute the expected mass density of metals and the mass density of remnant VMBHs produced in such a first episode of star formation. For a collapsed dark matter halo of total mass M , the associated baryonic mass is assumed to be $M(\Omega_B/\Omega_M)$ (where Ω_B/Ω_M is simply the baryon fraction). Following the results of Bromm *et al.* (2001), we assume that 1/2 of the total available gas is utilized in star formation, the rest remaining in diffuse form.

The relative mass fraction of $\text{SN}_{\gamma\gamma}$ and VMBH progenitors are parametrized as follows:

$$\begin{aligned} M_{\gamma\gamma} &= f_{\gamma\gamma} \frac{M}{2} \left(\frac{\Omega_B}{\Omega_M} \right) = f_{\gamma\gamma} M_* \\ M_{\bullet} &= (1 - f_{\gamma\gamma}) \frac{M}{2} \left(\frac{\Omega_B}{\Omega_M} \right) = (1 - f_{\gamma\gamma}) M_* \end{aligned} \quad (5)$$

where $M_{\gamma\gamma}$ (M_{\bullet}) is the total mass which ends up in $\text{SN}_{\gamma\gamma}$ (VMBHs) and M_* is the mass processed into stars. Thus, only a fraction f of the formed stars can contribute to gas metal enrichment. The metal yields for the dominant elements have been computed using the results of Heger & Woosley (2001), and are plotted in Fig. 3 as a function of the mass of the progenitor star. The bulk of the yield is contributed by O^{16} and the mass of metals ejected can be written as

$$M_Z \approx M_{\gamma\gamma}/2 - 10M_{\odot}. \quad (6)$$

Next, the further assumption is made that metals are ejected from the parent galaxy into the IGM and their cosmic volume filling factor is close to unity, therefore uniformly polluting the IGM. This comes from the results of Madau, Ferrara & Rees (2001) and Mori, Ferrara & Madau (2001), where it is shown that for reasonable values of the star formation efficiency, metal bubbles produced by (standard SNII in) proto-galaxies which result from 2σ peaks of the density power spectrum at redshift 10 do overlap. Indeed, the kinetic energy released by $\text{SN}_{\gamma\gamma}$ is much higher than for ordinary SNII (see Fig. 2), hence making our assumption even more solid.

As long as the average metallicity is below the critical value, *i.e.* $Z_{\text{cr}} = 10^{-5}Z_{\odot}$, we argue that the IMF remains top-heavy and the redshift-dependent critical density of metals contributed by $\text{SN}_{\gamma\gamma}$ can be computed,

$$\Omega_Z(z) = \frac{1}{\rho_{\text{cr}}(1+z)^3} \int_z^{\infty} dz' \int_{M_{\text{min}}(z')} dM n(M, z') M_Z \quad (7)$$

where $n(M, z)$ is the number density of halos per unit mass predicted by the Press-Schechter formalism and the integration is performed from $M_{\text{min}}(z)$ which is the minimum mass that can cool within a Hubble time at the specified formation redshift z , *i.e.* $t_H(z) \gtrsim t_{\text{cool}}(M, z)$ (see Ciardi *et al.* 2000). We adopt a cosmological model with the following parameters to compute the abundance of halos : $\Omega_M = 0.3$, $\Omega_{\Lambda} = 0.7$, $h = 0.65$, $\Omega_B = 0.047$ (latest predictions from BBN, see Burles, Nollett & Turner 2001) and use the COBE-normalized

power spectrum for fluctuations as described in Efstathiou, Bond & White (1992).

From the above expression, we can estimate the transition redshift z_f at which the mean metallicity is $10^{-5}Z_\odot$,

$$\langle Z(z_f) \rangle = \frac{\Omega_Z(z_f)}{\Omega_B} \approx 10^{-5}Z_\odot \quad (8)$$

for various values of the fraction $f_{\gamma\gamma}$. The results are plotted in Fig. 4 alongwith the corresponding critical density Ω_{VMBH} contributed by the VMBHs formed, which is given by,

$$\Omega_{VMBH}(z_f) = \frac{(1 - f_{\gamma\gamma})}{\rho_{\text{crit}}(1 + z_f)^3} \int_{z_f}^{\infty} dz' \int_{M_{\min}(z')} dM n(M, z') M_* \quad (9)$$

Several assumptions as to the fate of these VMBHs at late times will be examined in an attempt to obtain constraints on the value of $f_{\gamma\gamma}$ from current observations in the next Section.

4. Observational Constraints

The objective now is to set some limits on $f_{\gamma\gamma}$, the fraction of stars formed that result in $\text{SN}_{\gamma\gamma}$ providing the first metals, that are eventually responsible for the shift to a normal IMF. In order to compare the predicted critical density of VMBH remnants to present observational data we need to make further assumptions about the fate of these VMBHs at late times.

The mass density contributed by remnant supermassive black holes Ω_{SMBH}^0 can be estimated observationally¹ from the demography of local galaxies (Magorrian et al. 1998; Merritt & Ferrarese 2001). There are two extreme possibilities (bounding cases for the

¹The superscript 0 denotes the present day value

values of $f_{\gamma\gamma}$) concerning the relation between the inferred mass density of SMBHs and VMBHs:

- [A] $\Omega_{VMBH}(z_f) = \Omega_{SMBH}^0$: all VMBHs have, during the course of galaxy mergers, in fact, been used to build up the SMBHs detected today;
- [B] $\Omega_{VMBH}(z_f) = \Omega_{VMBH}^0 \neq \Omega_{SMBH}^0$ there is no relation between the detected SMBHs and the early VMBHs, implying that SMBHs have grown primarily by gas accretion.

Thus, in the first scenario [A], we assume that all VMBHs are able to sink to the center of host systems to merge within a Hubble time, giving birth to the SMBHs in the nuclei of galaxies that we see today. Note, that this is in fact unlikely (as explained further below), nevertheless, this argument provides an extreme bound.

It is important to point out here, that in the current proposed theoretical models for the mass accretion history of black holes, the mass density seen today locally in SMBHs can be built either predominantly by mergers or by accretion. In phenomenological models that attempt to tie in the current high redshift observations of the space density and luminosity function of quasars with that of the local space density of black holes wherein it is assumed that quasars are (*i*) powered by BHs and (*ii*) are optically bright for a period of $\approx 10^{6-7}$ yr (Haiman & Loeb 1998; Haehnelt, Natarajan & Rees 1998; Kauffmann & Haehnelt 2000), either picture (mergers/accretion) can adequately explain the mass assembly of the remnant SMBHs.

This permits both scenarios [A] (wherein SMBHs grow primarily via mergers of VMBHs during galaxy assembly) and [B] (wherein SMBHs grow primarily by accretion and Ω_{SMBH}^0 is unrelated to Ω_{VMBH}) to be plausible extreme cases. Consideration of cases [A] and [B] will provide bounds on the value for $f_{\gamma\gamma}$. For a given $f_{\gamma\gamma}$, the corresponding value for the transition redshift can be found on the z_f curve shown in Fig 4.

We note here that VMBHs in the mass range expected from the first episode of metal-free star formation (a few hundred solar masses) are likely to be ubiquitous. Using ISO observations, Gilmore & Unavane (1998) have convincingly argued that low mass stars (in fact hydrogen burning stars of any mass) do not provide a substantial portion of the dark matter inferred in the halos of galaxies. In combination with the mass limits obtained on potential dark matter candidates from the MACHO experiment (micro-lensing study) in our Galaxy (Alcock *et al.* 2001), low mass objects, with masses under $10 M_{\odot}$ are ruled out - thereby, making VMBHs ($\approx 100 M_{\odot}$ BHs) in halos (case [B]) plausible dark matter candidates.

For case [A], we can simply equate Ω_{VMBH}^0 to the measured mass density in SMBHs found from the demography of nuclei of nearby galaxies (Magorrian *et al.* 1998; Gebhardt *et al.* 2001) indicated by the horizontal line in Fig. 4 (top panel). The most recent value reported by Merritt & Ferrarese (2001) is $\Omega_{SMBH}^0 = 10^{-4}h\Omega_B$, which for $h = 0.65$ and $\Omega_B = 0.047$ yields $\Omega_{SMBH}^0 = 3.05 \times 10^{-6}$. From the top panel of Fig. 4, we see that this gives $f_{\gamma\gamma} \approx 0.009$. The corresponding value for the transition redshift can be found on the z_f curve on the same plot, yielding a value $z_f \approx 10$, which implies that a very small fraction of the mass involved in the first episode of star formation - approximately 1% - was processed into stars in the mass range $140 M_{\odot} < M_{\star} < 260 M_{\odot}$. The bulk of the mass, therefore, went in objects outside this range, yielding remnant black holes with mass $10 - 500 M_{\odot}$. The key point is that a very small amount of mass might have been processed into $SN_{\gamma\gamma}$. The scenario corresponding to [A] therefore implies that z_f , the transition redshift from top-heavy to normal IMF occurred at ≈ 10 . This value for z_f is consistent with the estimate from Madau, Ferrara & Rees (2001) for the redshift at which the metals in the Ly α forest need to have been released to explain their absorption line widths measured at $z \approx 3$ (their cool temperature requires ejection at much higher redshift).

Let us now look at the other extreme case [B], wherein the assembled SMBHs in galactic centers have formed primarily via accretion and are unrelated to VMBHs. This leads us to two further possibilities: (i) VMBHs would still be in the process of spiralling into the centers of galaxies due to dynamical friction but are unlikely to have reached the centers within a Hubble time due to the dynamical friction time-scale being long (Madau & Rees 2001), or (ii) VMBHs contribute the entire baryonic dark matter in galactic halos.

Pursuing scenario (i), therefore, at best some fraction of these VMBHs (for instance, those in gas-rich regions of gas-rich systems) might appear as off-center accreting sources that show up in the hard X-ray wave-band. Such sources have indeed been detected both by ROSAT (Roberts & Warwick 2000) and more recently by Chandra in nearby galaxies (M84: Jones 2001; NGC 720: Buote 2001).

In a survey of archival ROSAT HRI data to study the X-ray properties of the nuclei of 486 optically selected bright nearby galaxies (Ho, Filippenko & Sargent 1995), Roberts & Warwick (2000) found a large number of off-center X-ray sources. The X-ray sources detected within the optical extent of these galaxies were classified either as nuclear or non-nuclear (and therefore off-center) depending on whether the source was positioned within 25 arcsec of the optical nucleus. They detect a nuclear source in over 70% of the galaxy sample and a total of a 142 off-center sources. Roberts & Warwick (2000) find that the non-nuclear sources follow a steep, near power-law X-ray luminosity distribution in the $10^{36} - 10^{40}$ erg s⁻¹ which leads to an L_X/L_B ratio of

$$\frac{L_X}{L_B} = 1.1 \times 10^{39} \text{ erg s}^{-1} (10^{10} L_\odot)^{-1}. \quad (10)$$

The median luminosity of the non-nuclear sources is found to be a factor of ~ 10 lower than that of the nuclear sources. However, they estimate the incidence rate of off-center sources with $L_X \geq 10^{38.3}$ erg s⁻¹ (which corresponds to the Eddington luminosity for a 1.4 solar mass neutron star) to be ≈ 0.7 per $10^{10} L_\odot$ galaxy. The existence of accreting VMBHs

might also help explain the following observation. The far-IR excess detected with DIRBE at 60 and 100 μm has been tentatively interpreted as an extra-galactic background with integrated intensity of $44 \pm 9 \text{ nW m}^{-2}\text{sr}^{-1}$ in the range $60 - 100\mu\text{m}$ (Finkbeiner, Davis & Schlegel 2000). The energy required to produce such a FIR background could derive from a highly obscured population of accreting VMBHs at moderate redshifts (for an alternative to this see explanation of scenario (ii) below).

In order to estimate the mass density contributed by these VMBHs, we can compare the mass in VMBHs to that of the SMBH in a typical galaxy of luminosity say $10^{10} L_\odot$ for case [B]. Most of the VMBHs are likely to be en-route to galactic centers. Note however, that not all the inspiralling VMBHs will be accreting and be X-ray bright: many of these could, in fact, be low radiative efficiency ADAFs (Advection Dominated Accretion Flows), and therefore be too faint to be detected by ROSAT or Chandra or not accreting at all if they do not happen to be in gas-rich regions of the galaxy. Thus, using the following argument we can obtain a lower limit on the abundance of VMBHs.

The mass of the central SMBH hosted by a galaxy with a luminosity $L_{\text{galaxy}} = 10^{10} L_\odot$ (assumed to be the fiducial galaxy for these purposes) in the B-band is given by (Merritt & Ferrarese 2001):

$$M_{\text{SMBH}} = 10^{-3} M_{\text{bulge}} = 10^{-3} L_{\text{galaxy}}$$

where the mass-to-light ratio in the B-band is taken to be $1 M_\odot/L_\odot$ and the galaxy luminosity is essentially dominated by the bulge luminosity. Hence, the mass of the central SMBH is $M_{\text{SMBH}} \approx 10^7 M_\odot$. Now, we use the luminosity of the ROSAT off-center sources (Roberts & Warwick 2000) and use the fact that they find ≈ 0.7 off-center sources with luminosity $\geq 10^{38.3} \text{ erg s}^{-1}$ per $10^{10} L_\odot$ galaxy, to estimate the mass of VMBHs in the fiducial galaxy. If we assume that these VMBHs have a typical mass of $\approx 300 M_\odot$, their

Eddington luminosity is,

$$L_{\text{Edd}} = 4.3 \times 10^{40} \left(\frac{M_{VMBH}}{300 M_{\odot}} \right) \text{ erg s}^{-1}.$$

Thus, VMBHs appear to be radiating at sub-Eddington luminosities, the average rate (given by eq. 10) being $\approx 3\%$ of the Eddington value. This is consistent with the observed luminosities of the nuclear sources in the sample, which Roberts & Warwick (2000) find to be radiating at severely sub-Eddington rates.

Therefore, we expect that the typical accreting VMBH mass in a $10^{10} L_{\odot}$ galaxy to be about $210 M_{\odot}$. Little is known about the spatial distribution of such objects. How can we take into account the fact that only a fraction of the sources are likely to be accreting? Since the detected ROSAT off-center sources are within the optical radius of the galaxies, the number of non-accreting VMBHs in the halos of these galaxies can be large. One can obtain a simple estimate of this number by pursuing the following argument. Assume that VMBHs, being collisionless particles, closely trace the dark matter (which we take to obey a Navarro, Frenk & White [NFW, 1997] profile) and that the ratio of virial to optical radius is ≈ 15 for a $10^{10} L_{\odot}$ disk galaxy (Persic, Salucci & Stel, 1996). These hypotheses require that we scale up the total mass in VMBHs by a factor of ≈ 10 , which gives $M_{VMBH} = 2.1 \times 10^3 M_{\odot}$. Now, the ratio M_{VMBH}/M_{SMBH} is $\approx 2.1 \times 10^{-4}$, implying that $\Omega_{VMBH} = 2.1 \times 10^{-4} \Omega_{SMBH}^0 = 6.4 \times 10^{-10}$ which in turn gives $f_{\gamma\gamma} \approx 0.9$ (see dashed line in bottom panel of Fig. 4) and $z_f \gtrsim 16$.

Now we explore scenario (ii) of Case [B], the instance when VMBHs constitute the entire baryonic dark matter content of galaxy halos (but do not contribute to the disk dark matter). It is important to point out here that cosmological nucleosynthesis arguments require both baryonic and non-baryonic dark matter (Pagel 1990). Essentially, this is due to the fact that the mass density contributed by baryons Ω_B , is well in excess of Ω_V , the contribution to the mass density by visible baryons.

Using the luminosity dependent relation of visible to dark matter for spirals (Persic, Salucci & Stel, 1996) for a fiducial galaxy of $10^{10} L_\odot$ we find,

$$\frac{M_{vis}}{M_{DM}} \approx 0.05$$

where M_{vis} is the visible mass and $M_{DM} = M_{DM}^b + M_{DM}^{nb}$ is the total dark matter mass, given as a sum of a baryonic and a non-baryonic component. The total baryonic mass is a fraction Ω_B/Ω_M of the total mass of the system, *e.g.*

$$M_{vis} + M_{DM}^b = \frac{\Omega_B}{\Omega_M} (M_{vis} + M_{DM}).$$

From the two equations above and assuming a NFW density profile, we estimate that the total baryonic dark matter content as,

$$M_{DM}^b \simeq (\Omega_M^{-1} - 1) M_{vis} = 2.33 M_{vis};$$

moreover, 90% of this mass resides outside the optical radius and can be contributed by VMBHs:

$$\frac{M_{VMBH}}{M_{SMBH}} = \frac{2.1 \times M_{vis}}{10^{-3} \times M_{vis}} = 2.1 \times 10^3, \quad (11)$$

implying

$$\Omega_{VMBH} = 2.1 \times 10^3 \times \Omega_{SMBH} = 6.4 \times 10^{-3}. \quad (12)$$

Incorporating this constraint into Fig. 4 (bottom panel), we find $f_{\gamma\gamma} \approx 3 \times 10^{-6}$ and $z_f \gtrsim 2$. Note that this scenario does not violate the constraint on the over-production of background light (see Carr 1998; Bond, Carr & Hogan 1991; Wright et al. 1994). In fact, some fraction of the observed near-IR DIRBE excess could be produced by VMBHs. In a recent estimate of the cosmic background at $1.25 \mu\text{m}$ and $2.2 \mu\text{m}$ (corresponding to the J and K bands respectively) using 2MASS and the DIRBE results Cambresy et al. (2001), also find an excess (significantly higher than the integrated galaxy counts in the J and K bands) suggesting the contribution of other sources. Pop III stars and their VMBH remnants (accreting at very high redshifts) postulated here are likely candidates.

According to scenario [B], the average metal abundance at redshift $\gtrsim 4$ should be $Z_{\text{cr}} = 10^{-5} Z_{\odot}$, marking the transition from a top-heavy IMF to a standard power-law IMF. This does not necessarily violate the observed metal abundances in Damped Ly α systems, $Z \approx 10^{-3}$, as it is yet not clear to what extent the IGM metallicity is spatially uniform at these intermediate redshifts.

Therefore, scenario [B] is poorly constrained by the data, as the two options (i) and (ii) give large ranges for $f_{\gamma\gamma}$ and z_f : $3 \times 10^{-6} < f_{\gamma\gamma} < 0.9$ and $2 < z_f < 16$. Conversely, scenario [A] gives a lower limit on $f_{\gamma\gamma}$ and z_f : $f_{\gamma\gamma} > 0.009$ and $z_f > 10$.

The actual data do not allow us at present to strongly constrain the above two quantities, but they provide interesting bounds on the proposed scenario. These ranges also have implications for the expected detection rate of SNe beyond z_f with future instruments like the NGST (Marri & Ferrara 1998, Marri, Ferrara & Pozzetti 2000).

5. Discussion

We have proposed a scenario to solve a puzzling *star formation conundrum*: the first stars are now thought to be very massive and hence to lock their nucleosynthesis products into a remnant (very massive) black hole. This high-mass biased star formation mode continues as long as the gas remains metal-free. During this phase, metal enrichment can occur only if a fraction f of the stars have mass in the window leading to pair-unstable SNe ($140M_{\odot} < M_{\star} < 260M_{\odot}$) which disperse their heavy elements into the surrounding gas. Such metals enrich the gas up to $Z_{\text{cr}} \approx 10^{-5} Z_{\odot}$, when a transition to efficient cooling-driven fragmentation producing $\lesssim 1M_{\odot}$ clumps occurs at redshift z_f . We argue that the remaining fraction of the first stars end up in $\approx 100M_{\odot}$ VMBHs. By analyzing the evolutionary fate of such objects, we argue that [A] they could end up in the SMBHs

in the centers of galactic nuclei, [B] (i) could be en-route to the center and hence identified with the X-ray bright, off-center ROSAT sources, or (ii) constitute the entire baryonic dark matter content of galaxy halos. These possibilities are used to obtain constraints on the two quantities: $f_{\gamma\gamma} \gtrsim 0.09$ and $z_f \gtrsim 10$ for [A], and $f_{\gamma\gamma} \approx [10^{-5} - 0.9]$ and $z_f \approx [2 - 16]$ for case [B]. Interestingly, the range for z_f for case [A] is consistent with the estimate from Madau, Ferrara & Rees (2001) for the redshift at which the metals in the Ly α forest need to have been released to explain their absorption line widths measured at $z = 3$.

The value $Z_{\text{cr}} \approx 10^{-5} Z_{\odot}$ found here is admittedly somewhat uncertain. For this reason we have investigated how the above results might be affected by a different choice, *e.g.* assuming $Z_{\text{cr}} \approx 10^{-4} Z_{\odot}$. If the value for $f_{\gamma\gamma}$ is $\ll 1$, as implied by the SMBHs constraint or the upper bound from the baryonic halo shown in Fig. 4, the transition redshifts remain substantially unchanged (*i.e.* $z_f \approx 10$ and $\gtrsim 2$ respectively). However, higher values of Z_{cr} imply a more efficient metal enrichment and yield $f_{\gamma\gamma} \approx 0.1$ and $\approx 10^{-4}$, approximately a factor ten higher than for the standard case. Conversely, if $f_{\gamma\gamma} \approx 1$ as implied by the ROSAT constraint (see Fig. 4), then $f_{\gamma\gamma} \sim 0.9$ independent of the critical metallicity; a higher Z_{cr} results in a lower transition redshift, *i.e.* $z_f \approx 14$.

Several uncertainties remain in the comparison of the inferred density of VMBHs to local observations. For example, it is not obvious if SMBHs could at all form out of VMBHs. Dynamical friction can effectively drag VMBHs towards the center of the host system, at least within a distance of ~ 100 pc (Madau & Rees 2001). Unless most of the energy is radiated away in gravitational waves, it could be difficult for a VMBH cluster to coalesce into a single unit. Hence, the SMBH constraint should be interpreted as a strict upper bound on the critical density of VMBHs and therefore as a lower limit on $f_{\gamma\gamma}$ and z_f . Furthermore, accretion onto isolated VMBHs could be too inefficient to explain most of the off-center sources observed by ROSAT and CHANDRA. Higher accretion rates might

be activated by the tidal capture/disruption of ordinary stars. Question remains if the frequency of such an event is in fact sufficiently high to explain the data.

In spite of the many difficulties and uncertainties discussed above, our study represents a first attempt to link the first episode of cosmic star formation activity to present day observational evidence of their fossil remnants.

A top-heavy IMF for the early episodes of star formation in the universe might have other interesting observational consequences, we speculate further on them below. The kinetic energy released during the thermonuclear explosions powered by pair instability are $\approx 10^2$ larger than those of ordinary Type II SNe. This might cause the interaction with the circumstellar medium to be as strong as predicted for hypernovae (Woosley & Weaver 1982). However, these explosions do not lead to the ejection of strongly relativistic matter (Fryer, Woosley & Heger 2001) and therefore cannot power a gamma-ray burst (GRB).

In PopIII progenitors of VMBHs, the estimated angular momentum is sufficient to delay black hole formation and the system might develop triaxial deformations (Fryer, Woosley & Heger 2001). If the instabilities have enough time to grow, the core might break into smaller fragments that would then collapse and merge to form the central VMBH. If not, the star might still develop a bar-like configuration. Both these scenarios lead to a significant emission of gravitational waves (Schneider *et al.* 2000; Fryer, Holz & Hughes 2001). Furthermore, significant emission of gravitational radiation can occur as a result of the in-spiral and merger of VMBHs onto the SMBHs in the center of host systems (Madau & Rees, 2001)

Once the VMBHs have formed, accretion continues through a disk at a rate which can be as large as $10M_{\odot}\text{s}^{-1}$ (Fryer, Woosley & Heger 2001). Magnetic fields might drive an energetic jet which can produce a strong gamma-ray burst through the interaction with surrounding gas. The properties of these PopIII GRBs would be considerably different

from their more recent ($z < 5$) counterparts: depending on the uncertain interaction of the jet with the surrounding matter, the bursts would be probably longer [$10(1 + z)$ s] and the peak of emission, that in the rest frame is in γ -rays, would be shifted into X-rays. Indeed, BeppoSAX has revealed the existence of a new class of events, the so-called X-ray flashes or X-ray rich GRBs, which emit the bulk of their energy in X-rays (Piro, private communication). Furthermore, since PopIII GRBs explode at very high redshifts, it is likely that their optical afterglow might be heavily absorbed by the intervening gas. These systems might be the natural candidates for the significant number (about 40 % of GRBs for which fast follow-up observations were carried out) of GRBs which do not show an optical counterpart, the so-called GHOST (GRB Hiding Optical Source Transient) or dark GRBs. Other explanations ascribe the failed optical detection to dust extinction within the host system but the ultimate nature of GHOSTS is still very debated (Lazzati, Covino & Ghisellini, 2001; Djorgovski *et al.* 2001)

Finally, the energetic jets generated by GRBs engines produce, by photon-meson interaction, a burst of TeV neutrinos while propagating in the stellar envelope (Mészáros & Waxman 2001). The total integrated flux of TeV neutrinos from PopIII GRBs might be soon constrained by the AMANDA experiment (Schneider *et al.* 2001).

We are grateful to P. Coppi, R. Larson and M. Rees for comments and suggestions. We wish to thank V. Bromm and L. Piro for discussions. This work is partially supported (RS) by the Italian CNAA (Project 16/A); KO is supported by Research Fellowships of the Japan Society for the Promotion of Science for Young Scientists, grant 6819.

REFERENCES

Abel T., Anninos P., Norman M. L., & Zhang Y. 1998, ApJ, 518

Abel, T., Bryan, G. & Norman, M. 2000, ApJ, 540, 39

Alcock, C. *et al.* 2001, ApJ, 550, L169

Bond, J. R., Carr, B. J., & Hogan, C., 1991, ApJ, 367, 420

Bromm V., Coppi P.S., & Larson R.B., 1999, ApJ, 527, L5

Bromm V., Ferrara A., Coppi P.S., & Larson R.B., 2001, MNRAS, 328, 969

Buote, D., 2001, Proceedings of the Yale Workshop on galaxy shapes, ed. Natarajan, World-Scientific Publishers, New York

Burles, S., Nollett, K., & Turner, M. S., 2001, ApJ, 552, L1

Cambresy, L., Reach, W. T., Beichmann, C. A., & Jarrett, T. H., 2001, ApJ, 555, 563

Carr, B. J., Bond, J. R., & Arnett, W. D., 1984, ApJ, 277, 445

Carr, B. J., 1998, Phys. Rep., 307, 83

Ciardi, B., Ferrara, A. & Abel, T. 2000, ApJ, 533, 594

Ciardi, B., Ferrara, A., Governato, F., Jenkins, A., 2000, MNRAS, 314, 611

Djorgovski, S. G., Frail, D. A., Kulkarni S. R., Bloom J. S., Odewahn S. C., Diercks A., 2001, ApJ, submitted, (astro-ph/0107539)

Efstathiou, G. P., Bond, J. R., & White, S. D. M., 1992, MNRAS, 258, 1

El Eid, M. F., Fricke, K. J. & Ober, W. W. 1983, A&A, 119, 54

Finkbeiner, D., Davis, M., & Schlegel, D. J., 2000, ApJ, 544, 81

Fowler, W. A. & Hoyle, F. 1964, ApJS, 9, 201

Fricke, K. J. 1973, ApJ, 183, 941

Fryer, C. L., 1999, ApJ, 522, 413

Fryer, C. L., Woosley, S. E. & Heger, A., 2001, ApJ, 550, 372

Fryer, C. L., Holz D. E. & Hughes S. A., 2001, ApJ, submitted, (astro-ph/0106113)

Fuller, G. M., Woosley, S. E. & Weaver, T. A. 1986, ApJ, 307, 675

Gebhardt, K., Kormendy, J., Ho, L. C., et al., 2001, ApJ, 543, L5

Gilmore, G., & Unavane, M., 1998, MNRAS, 301, 813

Haehnelt, M., Natarajan, P., & Rees, M. J., 1998, MNRAS, 300, 817

Haiman, Z., & Loeb, A., 1998, ApJ, 503, 505

Haiman, Z., Thoul, A., & Loeb, A., 1996, ApJ, 464, 523

Heger, A. & Woosley, S. E., 2001, ApJ, in press, (astro-ph/0107037)

Hernandez, X. & Ferrara, A., 2001, MNRAS, 324, 484

Ho, L., Filippenko, A., & Sargent, W., 1995, ApJS, 98, 477

Jones, C., 2001, Proceedings of the Yale Workshop on galaxy shapes, ed. Natarajan, World-Scientific Publishers, New York

Kroupa, P. 2001, MNRAS, 322, 231

Larson, R. B., 1999, Proc. of Star Formation 1999, Ed. Nakamoto, Nobeyama Radio Observatory, 336

Lazzati, D., Covino, S. & Ghisellini, G., 2001, MNRAS, in press, (astro-ph/0011443)

Madau, P., Ferrara, A. & Rees, M. J. 2001, ApJ, 555, 92

Madau, P. & Rees, M. J. 2001, ApJL, 551, 27

Marri, S. & Ferrara, A. 1998, MNRAS, 317, 265

Marri, S., Ferrara, A. & Pozzetti, L. 2000, MNRAS, 317, 265

Merritt, D. & Ferrarese, L., 2001, MNRAS, 320, L30

Mészáros, P. & Waxman, E., 2001, Phys. Rev. Lett., 87, 171102

Mori, M., Ferrara, A., & Madau, P. 2001, ApJ, submitted (astro-ph/0106107)

Nakamura, F. & Umemura, M. 1999, ApJ, 515, 239

Nakamura, F. & Umemura, M. 2001, ApJ, 548, 19

Norris, J. E., Beers, T. C., & Ryan, S. G., 2000, ApJ, 540, 456

Oh, S.P., Haiman, Z., 2001, ApJ, submitted, (astro-ph/0108071)

Omukai, K. & Nishi, R. 1998, ApJ, 508, 141

Omukai, K. 2000, ApJ, 534, 809

Omukai, K. 2001, ApJ, 546, 635

Oh, S. P., Nollett, K. M., Madau, P. & Wasserburg, G. J. 2001, ApJL, submitted, (astro-ph/0109400)

Persic, M., Salucci, P. & Stel, F., 1996, MNRAS, 281, 27

Rees, M. 1976, MNRAS, 176, 483

Rees, M. J., & Ostriker, J. P., 1977, MNRAS, 179, 541

Ripamonti, E., Haardt, F., Ferrara, A. & Colpi, M. 2001, MNRAS, submitted, (astro-ph/0107095)

Scalo, J. 1998, The Stellar Initial Mass Function (38th Herstmonceux Conference), eds. G. Gilmore & D. Howell, ASP Conf. Series, 142, 201

Schneider, R., Ferrara, A., Ciardi, B., Ferrari, V., Matarrese, S., 2000, MNRAS, 317, 385

Schneider, R., Guetta, D., Ferrara, A. & Waxman, E., 2001, in preparation

Silk, J. 1977, ApJ, 211, 638

Silk, J. 1983, MNRAS, 205, 705

Spitzer, L., 1978, Physical processes in the interstellar medium, New York Wiley-Interscience.

Stahler, S. W., Shu, F. H. & Taam, R. E., 1980, ApJ, 241, 637

Uehara, H., Susa, H., Nishi, R. & Yamada, M., 1996, ApJ, 473, L95

Uehara, H., Inutsuka, S., 2000, ApJ, 513, L91

Wright, E. L. *et al.* 1994, ApJ, 420, 450

Wolfire, M. G., & Cassinelli, J. P. 1987, ApJ, 319, 850

Woosley, S. E. & Weaver, T. A., 1982, in Superovae: A Survey of Current Research, ed. M. Rees & R. J. Stoneham (Dordrecht: Reidel), 79

Woosley, S. E., & Weaver, T. A., 1995, ApJS, 101, 181

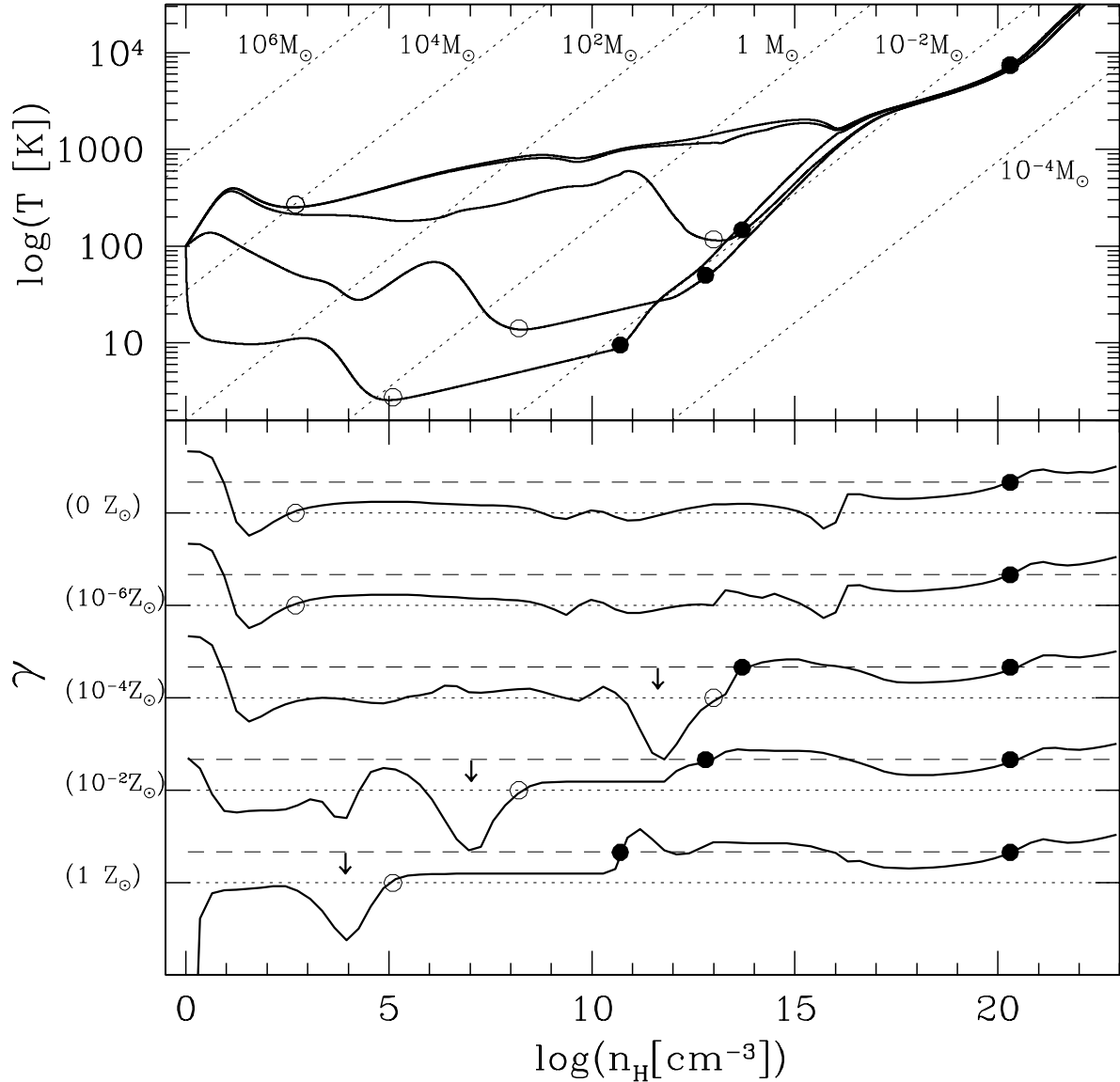
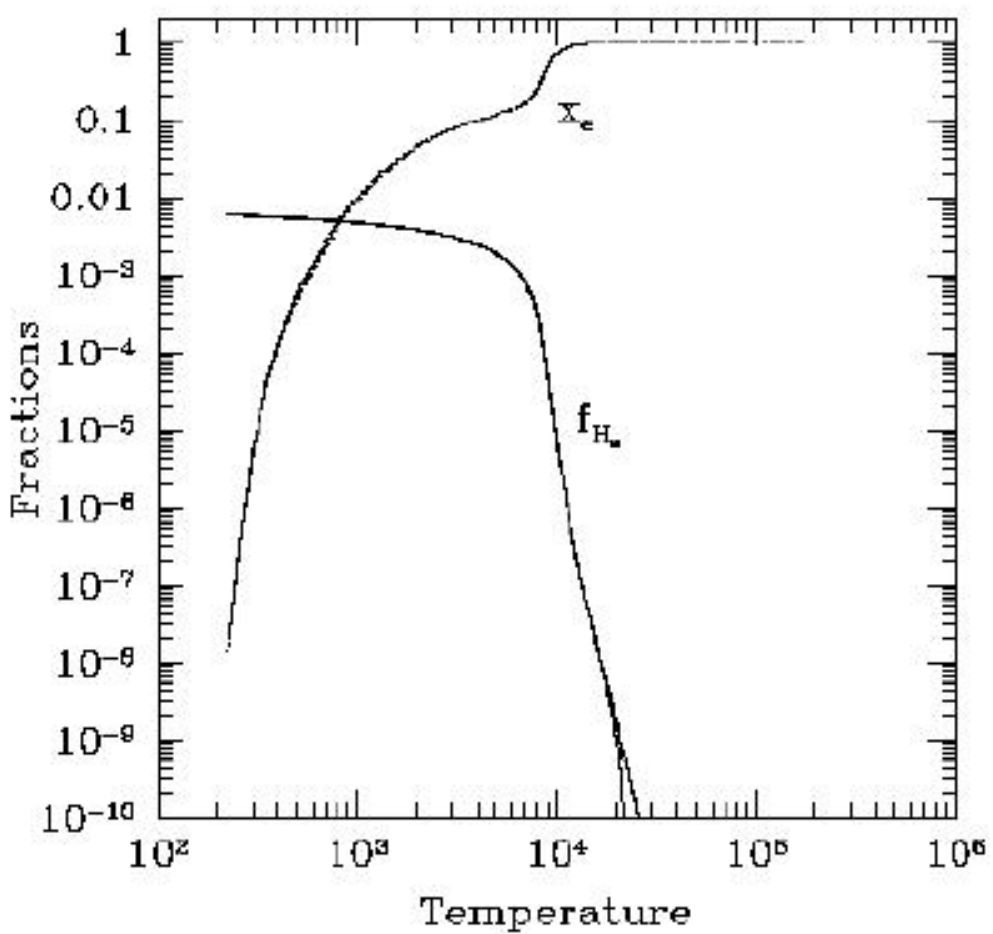


Fig. 1.— *Upper panel:* The evolution of the temperature as a function of the hydrogen number density of proto-stellar clouds with the same initial gas temperature but varying metallicities $Z = (0, 10^{-6}, 10^{-4}, 10^{-2}, 1) Z_\odot$ (Z increasing from top to bottom curves). The dashed lines correspond to the constant Jeans mass for spherical clumps; open circles indicate the points where fragmentation stops, filled circles mark the formation of hydrostatic cores. *Lower panel:* The adiabatic index γ as a function of the hydrogen number density for the curves shown in the upper panel. Dotted (dashed) lines correspond to $\gamma = 1$ ($\gamma = 4/3$); open and filled circles as above.



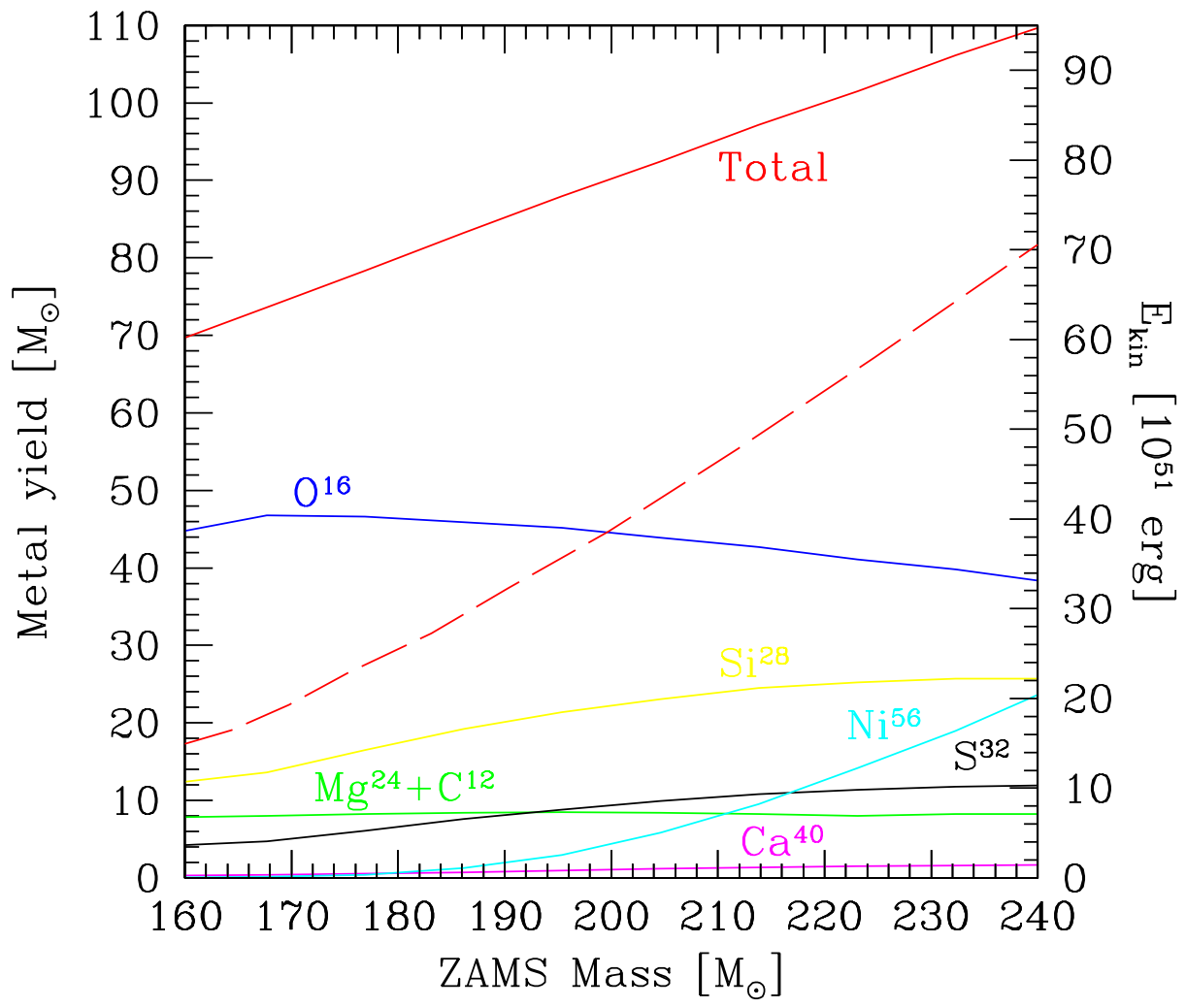


Fig. 3.— Metal yields of the main elements synthesized in metal-free $SN_{\gamma\gamma}$ according to Heger & Woosley (2001). The upper solid line corresponds to the total yield ejected and the dashed line indicates the kinetic energy of the explosion.

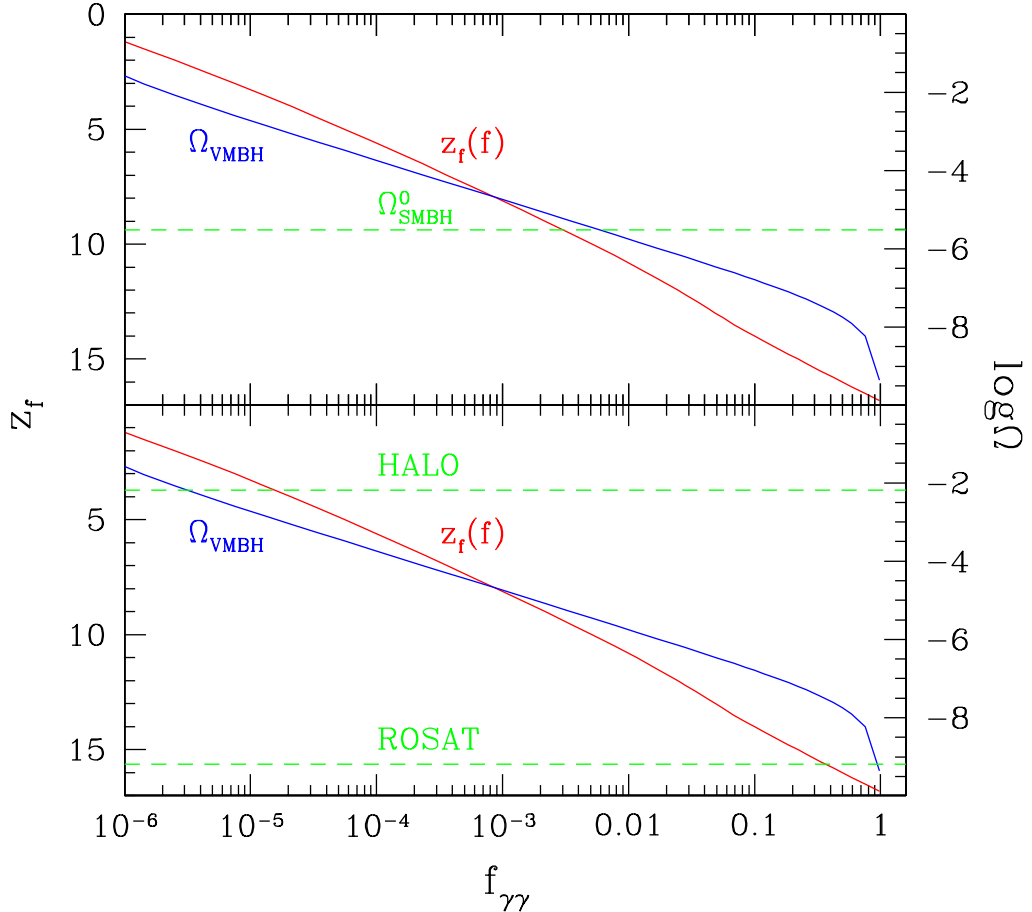


Fig. 4.— The top-heavy to normal IMF transition redshift, z_f , as a function of SN_{γγ} progenitor mass fraction and the mass density contributed by VMBHs Ω_{VMBH} . *Upper Panel*: The computed critical density of VMBH remnants is compared to the observed value for SMBHs (upper dashed horizontal line). *Lower Panel*: The computed critical density of VMBH remnants is compared to the contribution to Ω from the X-ray bright, off-center ROSAT sources (the lower dashed line) and to the abundance predicted assuming that the baryonic dark matter in galaxy halos is entirely contributed by VMBHs (upper dashed line). The observations on Ω_{VMBH} constrain the value for $f_{\gamma\gamma}$. For a given $f_{\gamma\gamma}$, the corresponding value for the transition redshift can be inferred by the z_f curve.